

Magnetic uniaxial alignment of the columnar superstructure of discotic metallomesogens over the centimetre length scale†

Ji-Hwan Lee,^a Sung-Min Choi,^{*a} Brian D. Pate,^{‡b} Malcolm H. Chisholm^b and Young-Soo Han^c

Received 15th March 2006, Accepted 2nd May 2006

First published as an Advance Article on the web 25th May 2006

DOI: 10.1039/b603902b

The uniaxial alignments of the columnar superstructure of discotic metallomesogens, cobalt octa(*n*-dodecylthio)porphyrazine (CoS12), over the centimetre length scale have been achieved by spinning samples under a static magnetic field. The orientations of the columnar superstructures were investigated by small angle neutron scattering (SANS) and cryogenic transmission electron microscopy (cryo-TEM). Upon cooling from the isotropic phase to the columnar mesophase in the presence of a static magnetic field (0.4–1.1 T), CoS12 formed oriented columnar superstructures with the columnar directors being isotropically distributed in the plane normal to the external magnetic field. When the samples were continuously spun during cooling in a static applied magnetic field of 1.0 T, CoS12 was observed to form uniaxially aligned columnar superstructures with the columnar domain directors being parallel to the rotation axis which was normal to the external field. The optimal rotation speed for the alignment was found to be as low as 5–10 rpm, where the full width at half maximum of the domain director distribution is minimized. The uniaxial alignments were achieved over a macroscopic length scale (*ca.* 1 cm). Cryo-TEM measurements revealed that the persistence length of the uniaxially aligned columns was at least 1 μm .

Introduction

Discotic liquid crystals (DLCs) have attracted substantial interest for their potential applications as photovoltaics,^{1,2} organic light emitting diodes,^{3,4} field effect transistors^{5,6} and sensors.^{7–9} The most basic class of DLC mesogens consists of a relatively rigid aromatic core with several more flexible aliphatic side chains. Depending on their specific molecular structure and thermodynamic state, DLCs have been found to exist in various phases such as nematic, hexagonal columnar and rectangular columnar.¹⁰ In the columnar phase, intermolecular π – π orbital overlap can be significant.^{11,12} Therefore, DLCs in a columnar mesophase often exhibit extremely anisotropic and order-dependent one-dimensional charge carrier mobility and photoconductivity along the columnar stacks, which are insulated from each other by their aliphatic peripheries.^{13–16} For many practical applications, however, unidirectional columnar domain alignment over a macroscopic length scale is critical.

While the alignment techniques for calamitic liquid crystals are well advanced, those for DLCs are still being developed, especially for the more highly ordered and viscous discotic columnar mesophases.¹⁷ In general, the alignment techniques for DLCs utilize interfacial interactions,^{18–24} photo induced alignment,²⁵ shear forces,²⁶ external fields,²⁷ temperature²⁸ and concentration gradients,²⁹ most of which are coupled with substrate effects. To our knowledge, however, there has been no example which demonstrates the uniaxial alignment of DLC columnar superstructure over the bulk length scale without relying on substrate effects.

Here, we report on an easy and simple method to control the orientation of the columnar DLC in a uniaxial manner over the centimetre length scale without relying on the substrate effects. This method utilizes the diamagnetic interaction of the aromatic core of DLCs with an external magnetic field, which involves continuous sample spinning in the presence of an external magnetic field while the sample is cooled from the isotropic phase to its liquid crystalline phase. The columnar orientations were directly observed by small-angle neutron scattering (SANS) and cryogenic transmission electron microscopy (cryo-TEM). To our knowledge, this is the first demonstration, using both reciprocal- and real-space imaging, of the use of magnetic fields to produce uniaxially aligned metal-containing DLCs in bulk length scale.

Magnetic alignment is one of the most straightforward and efficient methods to produce molecular materials ordered over bulk length scales. In almost all circumstances, the coupling energy between an isolated anisotropic molecule and an applied magnetic field H is very small relative to thermal energy. Therefore, an isolated molecule would show no magnetic alignment even upon application of very strong

^aDepartment of Nuclear and Quantum Engineering, Korea Advanced Institute of Science and Technology, Daejeon, 305-701, Republic of Korea. E-mail: sungmin@kaist.ac.kr; Fax: +82 42 869 3810; Tel: +82 42 869 3822

^bDepartment of Chemistry, The Ohio State University, Columbus, OH 43210, USA

^cHANARO Center, Korea Atomic Energy Research Institute, Daejeon, 305-353, Republic of Korea

† Electronic supplementary information (ESI) available: SANS instrument configurations, POM and XRD measurements, temperature dependence of magnetic alignment measured by SANS. See DOI: 10.1039/b603902b

‡ Present address: Department of Materials Science and Engineering, Institute for Soldier Nanotechnologies, Massachusetts Institute of Technology, Cambridge, MA 02139, USA.

magnetic fields. Rather, molecular alignment in DLCs is a domain phenomenon, and N molecules contained in a macroscopic domain essentially respond as a unit. The free energy of magnetic alignment for such a system can be expressed as^{30,31}

$$\Delta G_{\text{align}} = -\frac{1}{2} \Delta\chi (H \cdot n)^2 \quad (1)$$

where $\Delta\chi$ is the anisotropy of magnetic polarization and n is the columnar director. The free energy, therefore, can be minimized by adjusting the angle between H and n , inducing magnetic alignment. When $\Delta\chi < 0$, which is the case for almost all DLCs due to the large diamagnetic anisotropy of the aromatic core, the columnar director aligns normal to the applied magnetic field.

In the absence of an external magnetic field, the columnar directors of DLC domains are randomly oriented (Fig. 1a). When a static magnetic field is applied, they align with their directors normal to the applied field. Within the plane normal to the field, however, the columnar directors are randomly distributed (Fig. 1b). Application of a static magnetic field alone, therefore, does not produce uniaxial alignment over a bulk length scale for most columnar DLCs.

Upon application of a rotating magnetic field, the only columns with their directors normal to the field are those parallel to the axis of field rotation—thus this is the sole preferred domain orientation, and uniaxially aligned columnar DLC phases may be produced (Fig. 1c). The same effects can be achieved by simply rotating the sample in a static applied magnetic field with the rotation axis normal to the field, which is the method employed in this study. In this case, the columnar directors will align parallel to the rotation axis.

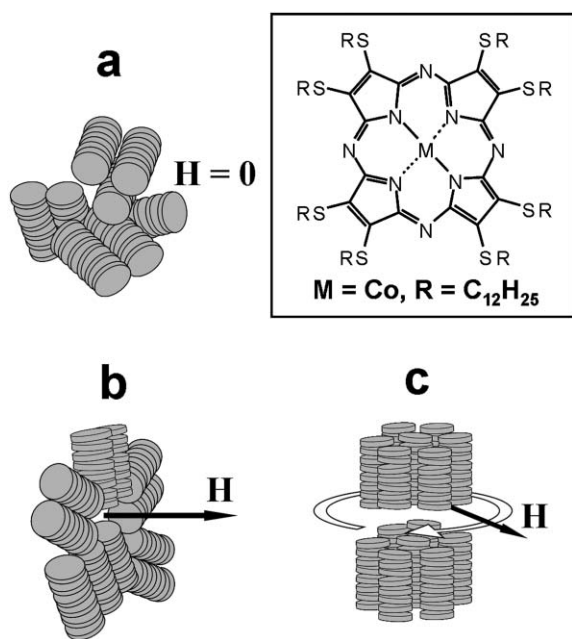


Fig. 1 A concept of the uniaxial alignment using a rotating magnetic field H . The schematics of columnar domain distributions, (a) in the absence of an applied magnetic field, (b) in the presence of an applied static magnetic field, and (c) in the presence of a rotating magnetic field are described. The inset shows the molecular structure of the DLC used in this study (CoS12).

Metal-containing discotic mesogens are currently of great interest due to the advantageous combined properties of liquid crystals and transition metals.^{31–36} In a previous study by Pate *et al.*,³¹ the responses of a series of octa(n -alkylthio) metalloporphyrazine DLCs (MS x , $M = \text{Co}, \text{Ni}, \text{Zn}, \text{Cu}$, n -alkyl = $\text{C}_x\text{H}_{2x+1}$, $x = 10$), which exhibit hexagonal columnar mesophases, to external magnetic fields were investigated. SANS measurements of NiS10 and ZnS10 revealed that the columnar directors orient perpendicular to applied static magnetic fields as low as 0.5 T when the samples were cooled from their isotropic phases. The threshold aligning field for CoS10 was found to be half that of NiS10 and ZnS10 while CuS10 exhibited no preferred alignment at fields as high as 1.02 T. These differences among the metalloporphyrazines were attributed to the competition of the diamagnetic moments of the aromatic cores and the paramagnetic moments of metal centers. In the case of CoS10, both moments work constructively enhancing magnetic alignment. In this previous study, however, only static magnetic fields were used and uniaxial alignment was not investigated.

In this study, we employed cobalt 2,3,7,8,12,13,17,18-octa(n -dodecylthio)porphyrazine (CoS12, the inset of Fig. 1) to demonstrate the uniaxial alignment of the columnar superstructures of DLCs by spinning the sample in a static magnetic field with the rotation axis normal to the field.

Experimental

Materials

Cobalt 2,3,7,8,12,13,17,18-octa(n -dodecylthio)porphyrazine (CoS12) was purchased from INNO BioSystem, which utilizes an analog of the synthetic procedure which is described elsewhere.^{36,37}

Instrumentation and measurements

Differential scanning calorimetry (DSC) measurements were performed in a nitrogen atmosphere using a Dupont 2010 DSC instrument at a scanning rate of $10\text{ }^\circ\text{C min}^{-1}$. The instrument was calibrated with an indium standard.

Polarized optical microscopy (POM) measurements were performed using a Olympus BX51 polarized optical microscope. Sample temperatures were controlled using a Mettler FP82 hot stage at a scanning rate of $1\text{ }^\circ\text{C min}^{-1}$.

Small angle neutron scattering (SANS) measurements were performed using the 30 m instruments (NG3 and NG7) at the NIST Center for Neutron Research (NCNR) in Gaithersburg, MD, USA and the 8 m SANS instrument at the High-flux Advanced Neutron Application Reactor (HANARO) of the Korea Atomic Energy Research Institute in Daejeon, Korea. The instrument configurations employed at HANARO and NCNR are summarized in the supplementary information. The scattering intensities were measured using a 2D detector as a function of scattering vector Q , $|Q| = 4\pi\sin\theta/\lambda$ where λ is the wavelength and 2θ is the scattering angle. The Q range used in this study was 0.025 \AA^{-1} – 0.48 \AA^{-1} . Scattering from the samples was corrected for background and empty cell scattering. All the collected data sets were circularly or annularly averaged using data reduction software provided by the NCNR.³⁸

To implement the rotation of CoS12 during cooling under a static magnetic field, a device which can control the sample rotation speeds (0–1000 rpm) and temperature (room temperature ~ 300 °C) was fabricated, having two orthogonal sample positions. This device was made of a non-magnetic material (aluminium) and placed between the poles of an electromagnet (HV7W, Walker Scientific Inc.) with a 62 mm pole gap, providing field strengths of up to 1.1 T.

In order to understand the three-dimensional structures of magnetically aligned columnar DLCs, it was necessary to perform SANS measurements in two or three orthogonal directions for each sample environment. Each sample was loaded in its isotropic phase to either (a) a disk-shaped cell (1.6 cm in diameter and 0.1 cm in thickness or beam path length) enclosed by two quartz disc windows or (b) a rectangular quartz cell (0.3 cm \times 0.3 cm \times 1.5 cm). Since the disk-shaped cell allows SANS measurements only through the thin direction due to limited neutron transmission, we employed a few combinations of sample loading directions against the magnetic field and neutron beam direction, as needed. For the SANS measurements intended to interrogate the effects of a static applied magnetic field, two disk-shaped cells containing the same material were loaded in two orthogonal positions (Fig. 2a). While the sample in position A was measured as loaded with the incident neutron beam N perpendicular to the direction of the applied magnetic field H ($N \perp H$), the sample in position B was rotated 90 degrees after magnetic alignment and then measured, allowing the incident neutron beam to be parallel to the direction that the field had been applied ($N \parallel H$, Fig. 2c). The samples prepared by spinning in the presence of the applied magnetic field (Fig. 2b), were measured in a similar way. During the measurements the magnetic field was turned off and the sample spinning was stopped. In addition to the measurements with the disk-shaped cells, a few experiments were performed with the rectangular cells, which allowed measurements for two orthogonal directions of the same specimen.

Cryo-TEM measurements were performed at -170 °C using a 120 kV Carl Zeiss EM912 OMEGA cryo-TEM at the Korea Basic Science Institute (KBSI). The samples aligned in bulk were cut into ~ 70 nm thick films using a Leica UCT ultramicrotome equipped with a FCS cryostage.

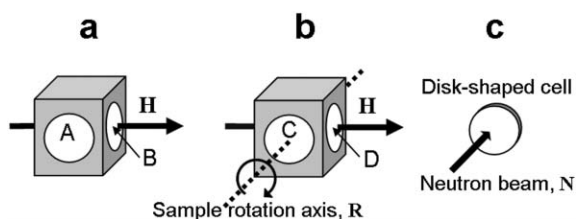


Fig. 2 Two orthogonal sample loading positions of the rotating/heating device. (a) The samples loaded at A and B were used for the SANS measurement with $N \perp H$ and $N \parallel H$, respectively. (b) Those at C and D were used for the SANS measurement with $N \parallel R$ and $N \perp R$, respectively. (c) The disk-shaped cell (16 mm in diameter and 1 mm beam path length) is enclosed by two quartz discs separated by titanium spacers.

Results and discussion

Phase behavior

Phase transitions of CoS12 were identified from DSC, POM and SANS measurements during heating and cooling. The transition temperatures determined from the DSC measurements during heating (cooling) with a scanning rate of 10 °C min^{-1} were 80 °C (51 °C) for the solid to the liquid crystalline phase and 127 °C (116 °C) for the liquid crystalline to the isotropic phase, respectively. The focal conic texture of the typical columnar hexagonal liquid crystalline phase was observed in the mesophase (see ESI†). Representative SANS patterns of CoS12, measured during the second heating, are shown in Fig. 3. The scattering peak in the high-temperature phase was very broad, which is typical of disordered liquids and may be assigned to a mean intermolecular spacing of 24.1 Å. The peak in the LC phase is relatively sharp, which is consistent with the higher degree of order associated with the hexagonal columnar liquid crystalline lattice. The inter-columnar distance a ($a = d/\cos 30^\circ$ for a hexagonal system, where d is the lattice spacing of the (100) plane) determined from the peak position of the LC phase was 27.9 Å. In the solid phase of CoS12, the SANS intensity showed three peaks which can be indexed with a $P2$ plane group (ESI†).

Magnetic alignment

The SANS measurements showed that CoS12 exhibits substantial preferred orientation when cooled from the isotropic phase to the columnar liquid crystalline phase in the presence of a static external magnetic field. The SANS patterns from the intercolumnar interferences become markedly anisotropic, which became increasingly pronounced as the temperature was decreased within the liquid crystalline range (ESI†). The results for CoS12 which were measured after cooling to the solid phase at room temperature are shown in Fig. 4.

The SANS pattern measured in the absence of an external magnetic field exhibited a sharp peak with isotropic distribution about the annular angle (Fig. 4a). This indicates that the bulk DLC system consists of a large collection of ordered

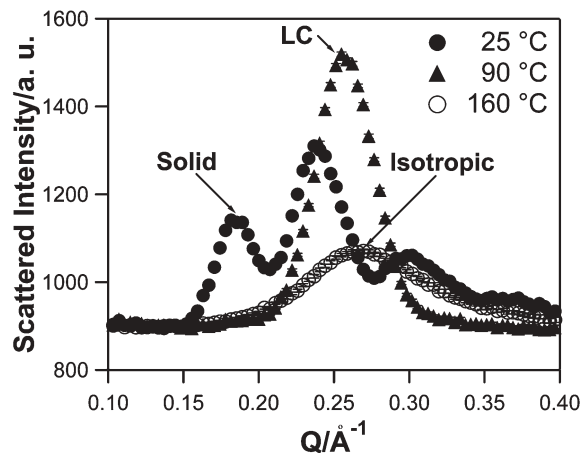


Fig. 3 SANS intensities of CoS12 at different phases. The measurements were performed upon heating.

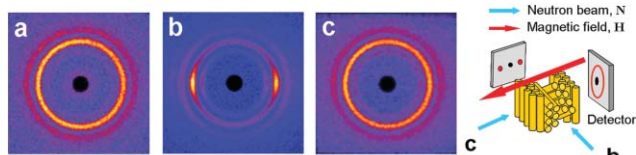


Fig. 4 Two-dimensional SANS patterns for CoS12 with/without an applied magnetic field. The samples were cooled from the isotropic phase down to the solid phase (a) in the absence and (b),(c) in the presence of the applied magnetic field of 1.0 T. For (b), $N \perp H$ and for (c), $N \parallel H$. The inset describes the induced orientations of the columnar directors and the SANS measurement conditions.

columnar domains with random orientations, similar to polycrystals. On the other hand, the SANS pattern measured in the presence of the applied magnetic field was distinctly anisotropic with the intensity maxima along the field direction (Fig. 4b). This clearly indicates that the domain directors, which are parallel to the columnar directors, are aligned normal to the applied field. When the sample was measured from an orthogonal direction, *i.e.* $N \parallel H$, as depicted in the inset of Fig. 4, a completely isotropic SANS pattern was observed (Fig. 4c). Thus, although the domain directors are constrained to lie normal to the applied field vector, they are uniformly distributed within this plane.

The response of CoS12 to a series of applied magnetic field strengths was measured. Each sample was first heated to 160 °C, well into its liquid phase, at which point the diffraction pattern was confirmed to be broad and isotropic. The applied external magnetic field was then adjusted to the desired strength, and the sample was cooled to 90 °C, well into its liquid crystalline phase. The cooling rate was approximately 5 °C min⁻¹. After allowing a time of 5 minutes for equilibration, SANS measurements were performed. These steps were repeated for different field strengths. The two-dimensional SANS data were annularly averaged at $Q = 0.26 \text{ \AA}^{-1}$ for the liquid crystalline phase. The annularly averaged SANS data, $I(\phi)$, were fitted with a Lorentzian function as shown in the inset of Fig. 5. The full width at half maximum (FWHM) of $I(\phi)$ as a function of the applied field strength is shown in Fig. 5. The diffraction anisotropy was apparent at fields as low as 0.296 T. As the field strength increased, the FWHM rapidly decreased at low fields and then asymptoted to about 40°. The saturating magnetic field for the alignment of CoS12 was as low as ~0.6 T which is much lower than those for other DLCs.^{16,17} This is attributed to the constructive effects of the diamagnetic moments of the aromatic core and the paramagnetic moments of the central cobalt atom of CoS12.³¹

Magnetic uniaxial alignment

Uniaxial alignment of CoS12 was obtained by cooling and rotating samples from the isotropic phase in the presence of an applied magnetic field of 1.0 T. The rotation axis was perpendicular to the magnetic field direction, and a series of rotation speeds was tested. Once the sample was fully cooled to the solid phase with a cooling rate of approximately 5 °C min⁻¹, the sample was removed from the rotation/heating device, and then SANS measurements were performed for two orthogonal directions of the sample, as shown in the inset of

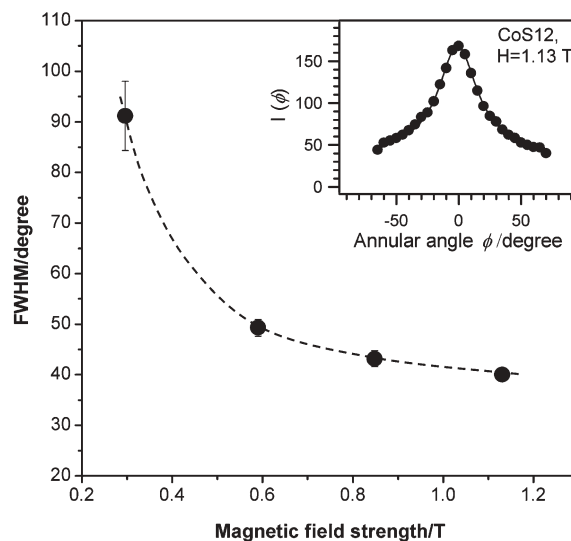


Fig. 5 The FWHM of the annularly averaged SANS data of CoS12 as a function of the applied magnetic field strength. The inset shows a Lorentzian fit for the SANS data of CoS12 cooled from the isotropic phase under $H = 1.13 \text{ T}$. The measurements were performed at 90 °C at which the samples are in their columnar liquid crystalline phases.

Fig. 6. During these SANS measurements, no magnetic field was applied.

The SANS pattern (Fig. 6a), which was measured with the neutron beam direction perpendicular to the rotation axis, shows a very sharp anisotropy. On the other hand, the pattern, which was measured with the neutron beam direction parallel to the rotation axis, shows an isotropic scattering distribution (Fig. 6b). These results clearly indicate that the columnar domains are uniaxially aligned parallel to the sample rotation axis which is perpendicular to the applied field. These measurements were performed for samples filled in two disk-shaped cells loaded at two orthogonal positions in the rotation/heating device (Fig. 2). To measure the sample from another orthogonal direction, the sample was filled in a rectangular sample cell and rotated as described in the inset of Fig. 6. The SANS patterns measured from two orthogonal directions, each normal to the sample rotation axis, are both strongly anisotropic (Fig. 6c and 6d). This further confirms the uniaxial alignment of CoS12. It should be noted that the anisotropic SANS patterns were obtained from the samples filled in the disk-shaped cells of 0.1 cm thick and 1.6 cm in diameter, using a neutron beam of 1.0 cm in diameter at the sample. Therefore, an ensemble averaged uniaxial alignment of CoS12 over a bulk length scale of *ca.* 1.0 cm was achieved in this study. To our best knowledge, this is the largest uniaxially aligned columnar metal-containing DLC in bulk ever reported. This alignment has a very slow relaxation time in the solid phase. SANS patterns measured after about three months did not show any appreciable changes.

The uniaxial alignments were tested with various sample rotation speeds, for CoS12 in the presence of an applied field of 1.0 T. In all the cases, the incident neutron beam was positioned perpendicular to the sample rotation axis, resulting in anisotropic SANS patterns similar to that seen in Fig. 6a. The scattered neutron intensity, $I(\phi)$ which is annularly

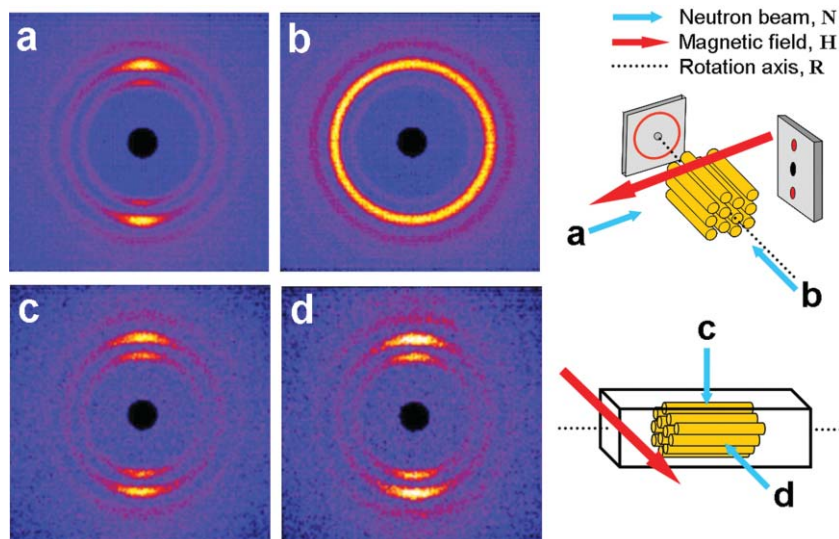


Fig. 6 Two-dimensional SANS patterns of uniaxially aligned CoS12. The samples were spun at 5 rpm in the presence of an applied magnetic field of 1.0 T while being cooled from the isotropic phase to the solid phase. The measurements were performed at room temperature, *i.e.* the solid phase. The inset describes the induced orientations of the columnar directors and the neutron beam directions against the sample orientation during SANS measurements.

averaged at the highest peak position ($Q = 0.24 \text{ \AA}^{-1}$) shows a very sharp anisotropy as depicted in the inset of Fig. 7. Fitting the annularly averaged SANS data with a Lorentzian function, the FWHM values of the columnar domain mosaic distribution as a function of the sample rotation speed were obtained. To achieve uniaxial alignment, the rotation speed must be higher than the inverse of re-orientational relaxation time of columnar domains under an applied magnetic field. We expected that the FWHM values would decrease with the rotation speed and reach an asymptote above a certain threshold speed. However, as the rotation speed increased, the FWHM decreased initially but, after reaching the lowest value 24.5° at 5–10 rpm, it slightly increased rather than

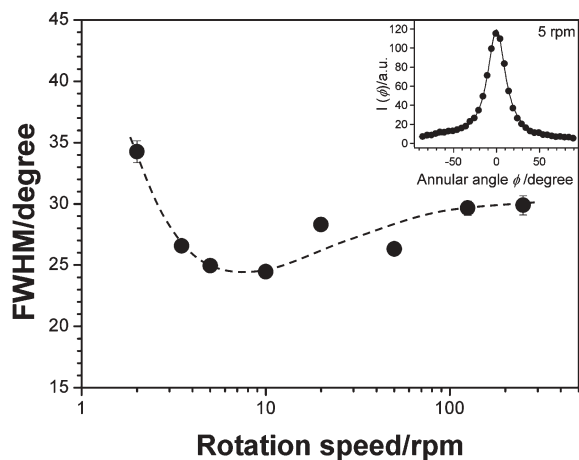


Fig. 7 The FWHM of the annular average of the uniaxially aligned CoS12 as a function of the sample rotation speed. The inset shows a Lorentzian fit for the SANS data of a 5 rpm sample. The magnetic field strength was set at 1.0 T and all the SANS measurements were performed after the samples were cooled from the isotropic phase down to the solid phase.

reaching an asymptote. The FWHM of the uniaxially aligned CoS12 was almost a factor 2 smaller than that of CoS12 aligned without sample spinning. The increase of the FWHM at higher rotation rates may be attributed to the disturbance induced by the combined effects of centrifugal force and imperfect sample filling in the cell. The sample cells were fully filled at the isotropic phase, but as the samples were cooled down to the liquid crystalline phase the mass density increased, producing small void space within the sample cell. Upon rotating the samples at high speed, we observed that these small voids became concentrated at the center of sample cells, which would disturb the nearby columnar alignments. The rotation rates of 5–10 rpm are quite slow and readily achievable. The uniaxial alignment method presented here provides for straightforward, non-invasive access to fabricating uniaxially aligned columnar discotic liquid crystal materials in over a bulk length scale.

The low magnification cryo-TEM micrographs of the uniaxially aligned CoS12 at 5 rpm, sectioned along two orthogonal directions, are shown in Fig. 8. While the image of the sample sectioned perpendicular to the sample rotation axis (Fig. 8a) shows no preferred direction, the image of the sample sectioned parallel to the sample rotation axis (Fig. 8b) shows a distinct preferred orientation axis which is parallel to the rotation axis. This further confirms the uniaxial alignment of CoS12 along the sample rotation axis. The high magnification cryo-TEM micrograph of the uniaxially aligned CoS12 at 5 rpm, the same specimen shown in Fig. 8b, reveals a single domain of highly aligned columns (Fig. 8c). This image, together with the images taken for neighboring regions of the sample, revealed that the linearity of each column was maintained up to *ca.* $1 \mu\text{m}$, which is close to the measurement limit. The linearity may persist somewhat beyond $1 \mu\text{m}$, corresponding to a stacking of more than 2200 molecules (intracolumnar spacing $\approx 4.5 \text{ \AA}$). The d-spacing, calculated

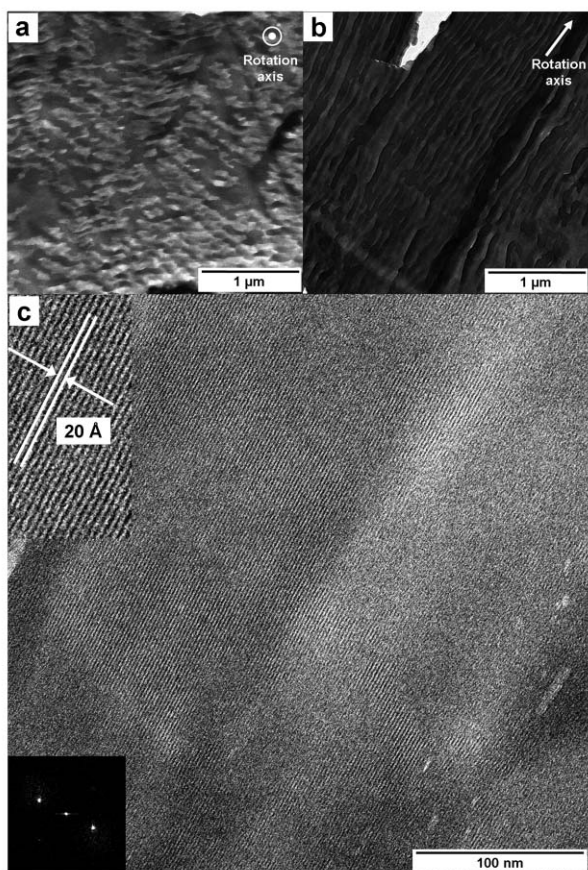


Fig. 8 Cryo-TEM micrographs of the uniaxially aligned CoS12. The sample was aligned at 5 rpm under an applied magnetic field of 1.0 T, and then sectioned in ~ 70 nm thickness along orthogonal directions, (a) parallel, (b) perpendicular to the sample rotation axis with low magnification and (c) parallel to the sample rotation axis with high magnification. The inset is the fast Fourier transform of the image. The average distance between two equal stripes is 20 Å.

from the fast Fourier transform (FFT) data of the image, was 20 Å, which agrees with the value (20.6 Å) measured by SANS.

Conclusions

The uniaxial alignments of the columnar superstructure of a discotic metallomesogen, CoS12, over the centimetre length scale have been achieved by spinning samples under a static magnetic field. To our best knowledge, this is the first demonstration, using both reciprocal- and real-space imaging, of the use of magnetic fields to produce uniaxially aligned metal-containing DLCs over the bulk length scale. When the samples were continuously spun during cooling in a static applied magnetic field of 1.0 T, CoS12 was observed to form uniaxially aligned columnar superstructures with the columnar domain directors being parallel to the rotation axis which was normal to the external field. The optimal sample rotation speed for CoS12 under our experimental conditions was found to be 5–10 rpm, where the FWHM of the domain director distribution was minimized. Cryo-TEM measurements showed that the persistence length of the columnar directors was at least 1 μm. Considering that these uniaxial alignments were

achieved over a macroscopic length scale (*ca.* 1.0 cm) using easily accessible magnetic field strengths and rotation speeds, the alignment method presented here can provide a straightforward means to fabricate uniaxially aligned columnar diamagnetic discotic liquid crystal materials in bulk length scale, which will facilitate the technological applications of DLCs for advanced molecular devices.

Acknowledgements

This work was supported by the program of the Basic Atomic Energy Research Institute (BAERI) which is a part of the Nuclear R&D Programs funded by the Ministry of Science & Technology (MOST) of Korea and the HANARO Utilization Program (M2-0363-00-0063). We thank the HANARO at KAERI and NCNR at NIST for SANS beamtime supports. The work utilized NIST facilities supported in part by the National Science Foundation under DMR-9986442. We also thank J.-K. Kim, S.-M. Kim and J.-Y. Lee at Korea Basic Science Institute (KBSI) for technical assistance during cryo-TEM measurements and J.-S. Lee for DSC and POM measurements.

References

- 1 L. Schmidt-Mende, A. Fechtenkötter, K. Müllen, E. Moons, R. H. Friend and J. D. MacKenzie, *Science*, 2001, **293**, 1119.
- 2 P. Samori, X. Yin, N. Tchebotareva, Z. Wang, T. Pakula, F. Jäckel, M. D. Watson, A. Venturini, K. Müllen and J. P. Rabe, *J. Am. Chem. Soc.*, 2004, **126**, 3567.
- 3 T. Christ, B. Glösen, A. Greiner, A. Kettner, R. Sander, V. Stümpflen, V. Tsukruk and J. H. Wendorff, *Adv. Mater.*, 1997, **9**, 48.
- 4 I. Seguy, P. Destruel and H. Bock, *Synth. Met.*, 2000, **111–112**, 15; I. Seguy, P. Jolinat, P. Destruel, J. Farenc, R. Mamy, H. Bock, J. Ip and T. P. Nguyen, *J. Appl. Phys.*, 2001, **89**, 5442.
- 5 A. M. Van De Craats, N. Stutzmann, O. Bunk, M. M. Nielsen, M. Watson, K. Müllen, H. D. Chanzy, H. Sirringhaus and R. H. Friend, *Adv. Mater.*, 2003, **15**, 495; W. Pisula, A. Menon, M. Stepputat, I. Lieberwirth, U. Kolb, A. Tracz, H. Sirringhaus, T. Pakula and K. Müllen, *Adv. Mater.*, 2005, **17**, 684.
- 6 F. Jäckel, M. D. Watson, K. Müllen and J. P. Rabe, *Phys. Rev. Lett.*, 2004, **92**, 188303.
- 7 C.-Y. Liu and A. J. Bard, *Nature*, 2002, **418**, 162.
- 8 N. Boden, R. J. Bushby, J. Clements and B. Movaghar, *J. Mater. Chem.*, 1999, **9**, 2081.
- 9 Y. Amao, K. Miyakawa and I. Okura, *J. Mater. Chem.*, 2000, **10**, 305.
- 10 R. J. Bushby and O. R. Lozman, *Curr. Opin. Colloid Interface Sci.*, 2002, **7**, 343.
- 11 D. Adam, P. Schuhmacher, J. Simmerer, L. Häussling, K. Siemensmeyer, K. H. Etzbach, H. Ringsdorf and D. Haarer, *Nature*, 1994, **371**, 141.
- 12 N. Boden, R. J. Bushby, J. Clements, B. Movaghar, K. J. Donovan and T. Kreouzis, *Phys. Rev. B: Condens. Matter*, 1995, **52**, 13 274.
- 13 P. G. Schouten, J. M. Warman, M. P. de Haas, M. A. Fox and H.-L. Pan, *Nature*, 1991, **353**, 736.
- 14 N. Boden, R. J. Bushby, J. Clements, M. V. Jesudason, P. F. Knowles and G. Williams, *Chem. Phys. Lett.*, 1988, **152**, 94; N. Boden, R. C. Borner, R. J. Bushby and J. Clements, *J. Am. Chem. Soc.*, 1994, **116**, 10807.
- 15 D. Adam, F. Closs, T. Frey, D. Funhoff, D. Haarer, H. Ringsdorf, P. Schuhmacher and K. Siemensmeyer, *Phys. Rev. Lett.*, 1993, **70**, 457; J. Simmerer, B. Glösen, W. Paulus, A. Kettner, P. Schuhmacher, D. Adam, K. H. Etzbach, K. Siemensmeyer, J. H. Wendorff, H. Ringsdorf and D. Haarer, *Adv. Mater.*, 1996, **8**, 815.
- 16 N. Boden, R. J. Bushby and J. Clements, *J. Chem. Phys.*, 1993, **98**, 5920.

- 17 S. H. Eichhorn, A. Adavelli, H. S. Li and N. Fox, *Mol. Cryst. Liq. Cryst.*, 2003, **397**, 47.
- 18 J. Y. Josefowicz, N. C. Maliszewskyj, S. H. J. Idziak, P. A. Heiney, J. P. McCauley, Jr. and A. B. Smith III, *Science*, 1993, **260**, 323.
- 19 P. Smolenyak, R. Peterson, K. Nebesny, M. Törker, D. F. O'Brien and N. R. Armstrong, *J. Am. Chem. Soc.*, 1999, **121**, 8628.
- 20 B. W. Laursen, K. Nørgaard, N. Reitzel, J. B. Simonsen, C. B. Nielsen, J. Als-Nielsen, T. Bjørnholm, T. I. Sølling, M. M. Nielsen, O. Bunk, K. Kjaer, N. Tchebotareva, M. D. Watson, K. Müllen and J. Piris, *Langmuir*, 2004, **20**, 4139.
- 21 H. Schönherr, F. J. B. Kremer, S. Kumar, J. A. Rego, H. Wolf, H. Ringsdorf, M. Jaschke, H.-J. Butt and E. Bamberg, *J. Am. Chem. Soc.*, 1996, **118**, 13051.
- 22 N. Boden, R. J. Bushby, P. S. Martin, S. D. Evans, R. W. Owens and D. A. Smith, *Langmuir*, 1999, **15**, 3790.
- 23 S. Zimmermann, J. H. Wendorff and C. Weder, *Chem. Mater.*, 2002, **14**, 2218.
- 24 O. Bunk, M. M. Nielsen, T. I. Sølling, A. M. Van de Craats and N. Stutzmann, *J. Am. Chem. Soc.*, 2003, **125**, 2252.
- 25 K. Ichimura, S. Furumi, S. Morino, M. Kidowaki, M. Nakagawa, M. Ogawa and Y. Nishiura, *Adv. Mater.*, 2000, **12**, 950.
- 26 D. H. Van Winkle and N. A. Clark, *Phys. Rev. Lett.*, 1982, **48**, 1407.
- 27 S. Ikeda, Y. Takanishi, K. Ishikawa and H. Takezoe, *Mol. Cryst. Liq. Cryst.*, 1999, **329**, 589.
- 28 C.-Y. Liu and A. J. Bard, *Chem. Mater.*, 2000, **12**, 2353.
- 29 A. Tracz, J. K. Jeszka, M. D. Watson, W. Pisula, K. Müllen and T. Pakula, *J. Am. Chem. Soc.*, 2003, **125**, 1682.
- 30 A. J. Dekker, *Can. J. Phys.*, 1987, **65**, 1185.
- 31 B. D. Pate, S.-M. Choi, U. Werner-Zwanziger, D. V. Baxter, J. M. Zaleski and M. H. Chisholm, *Chem. Mater.*, 2002, **14**, 1930.
- 32 G. Ricciardi, A. Rosa, I. Ciofini and A. Bencini, *Inorg. Chem.*, 1999, **38**, 1422; S. Belviso, G. Ricciardi and F. Lejl, *J. Mater. Chem.*, 2000, **10**, 297.
- 33 C.-Y. Liu, H.-L. Pan, M. A. Fox and A. J. Bard, *Science*, 1993, **261**, 897.
- 34 J. M. Fox, T. J. Katz, S. Van Elshocht, T. Verbiest, M. Kauranen, A. Persoons, T. Thongpanchang, T. Krauss and L. Brus, *J. Am. Chem. Soc.*, 1999, **121**, 3453.
- 35 J. Barberá, E. Caverio, M. Lehmann, J. Serrano, T. Sierra and J. T. Vázquez, *J. Am. Chem. Soc.*, 2003, **125**, 4527.
- 36 F. Lejl, G. Morelli, G. Ricciardi, A. Roviello and A. Sirigu, *Liq. Cryst.*, 1992, **12**, 941.
- 37 P. Doppelt and S. Huille, *New J. Chem.*, 1990, **14**, 607.
- 38 S. R. Kline, *SANS Data Reduction and Analysis version 4.2*, NIST Center for Neutron Research, Gaithersburg, MD USA, 2003.

Chemical Science

An exciting news supplement providing a snapshot of the latest developments across the chemical sciences



Free online and in print issues of selected RSC journals!*

Research Highlights – newsworthy articles and significant scientific advances

Essential Elements – latest developments from RSC publications

Free access to the original research paper from every online article

*A separately issued print subscription is also available

RSC Publishing

www.rsc.org/chemicalscience